JOURNAL OF THE PHYSICAL SOCIETY OF JAPAN, Vol. 29, No. 3, SEPTEMBER, 1970

Cyclotron Resonance in the Valence Band of Germanium under Uniaxial Stress

Hiroshi FUJIYASU,* Kazuo MURASE and Eizo OTSUKA
Department of Physics, Osaka University, Toyonaka, Osaka

(Received March 25, 1970)

The inverse mass parameters, deformation potential constants and g-factor of the valence band of germanium are determined through a cyclotron resonance study. By means of 35 and 70 GHz microwave spectrometers, several quantum lines are observed with good resolution between 1.5 and 4.2°K under the application of uniaxial compression along particular crystal axes. Analyses of these quantum lines yield: $A=-13.50\pm0.05$, $B=-8.80\pm0.09$ and $N=-35.20\pm0.23$ in the unit of $(\hbar^2/2m_0)$; the shear deformation potential constants $D_u=3.14\pm0.20$, $D_{u'}=4.00\pm0.20$ and the dilatational one $D_d^V=-5.2^{-0.5}_{+1.0}$ or $+3.3^{+0.5}_{-1.0}$ in the unit of (eV); while the g-value is found to be 7.8.

§ 1. Introduction

Cyclotron resonance is one of the most straightforward and precise techniques to determine the band parameters of solids. Supported by theoretical considerations, Lax, Zeiger and Dexter[1] and Dresselhaus, Kip and Kittel[2] played the pioneer roles in cyclotron resonance for unveiling the band structures of germanium and silicon.

The valence band is more complex than the conduction hand. Its band edge is located at $k=0$, or the Γ'_{25} point, in the Brillouin zone. This band has degeneracy due to the cubic symmetry and consequently the warped equipotential energy surfaces. The values of inverse mass parameters A, B and N can be obtained through measuring the cyclotron resonance peaks of the so-called light and heavy holes. Their precise determination, however, has been difficult, since the resonance line, especially that of heavy hole, is broadened on account of the so-called quantum effects. The Landau levels of the degenerate band are not of equal spacing, depending on the quantum number n and the wave number k_H along the applied magnetic field. In the absence of uniaxial stress, which lifts the Γ'_{25} point degeneracy, the quantum effects have been theoretically investigated by Luttinger and Kohn,[3] Luttinger,[4] Wallis and Bowlden,[5] while are experimentally observed first in cyclotron resonance of germanium by Fletcher *et al.*,[6] at 1.3°K. Goodman[7] compared their experimental results with Luttinger's theory.[4] Later Hensel[8] made

* Now at Faculty of Engineering, Shizuoka University, Hamamatsu.

more detailed experiments and Okazaki[9] successfully explained Hensel's new lines through a theoretical calculation which is more precise than Goodman's one.

The quantum-mechanical treatment of cyclotron resonance in the presence of band degeneracy is difficult and tedious, particularly so in the linewidth problem. Hensel and Feher[10] avoided the difficulty by applying uniaxial stress on silicon, followed by Hasegawa's theoretical interpretation.[11] Application of uniaxial stress removes the cubic symmetry from the crystal and thus lifts the Γ'_{25} point degeneracy. In zero magnetic field, the decoupled states are degenerate Kramers doublets designated by quantum numbers $\pm M_j$. The decoupled bands have nearly ellipsoidal surfaces which, like the conduction band, give cyclotron resonance masses amenable to a straight interpretation. On compression, $M_j=\pm\frac{3}{2}$ bands go down both for silicon and for germanium on account of the plus signs of the deformation potential constants. The band parameters A, B and N of silicon have been determined by Hensel and Feher more accurately than in earlier works. They used a 9 GHz microwave spectrometer, in which $\omega_c\tau$ is not large enough to resolve quantum lines even at 1.2°K. They obtained the deformation potential constants D_u and $D_{u'}$, analyzing the linewidth and position of the so-called split hole resonance which consist of different quantum transitions. In 1966 Hensel[12] and Otsuka, Murase and Fujiyasu[13] took the same procedure for germanium and observed several quantum lines at 50 GHz and 35 GHz, respectively. For germanium, analysis is simpler than for silicon because of a large spin-orbit coupling. Values of A, B and N as well as those of D_u and $D_{u'}$ have thus been obtained. Recently Hensel[14] observed combined resonance and determined the valence band g-factor precisely.

The uniaxial stress apparatus used in our earlier work was a kind of the so-called perpendicular squeezer with which the degree of freedom of the geometry is limited and hence not much analysis could be carried out. Success in making a parallel squeezer has enabled us to get more precise values of the above mentioned parameters. The linewidth of the primary quantum line ($n=0\rightarrow1$, $M_j=-\frac{1}{2}$) is measured as a function of temperature and the dilatational deformation potential constant D_d^V undetermined so far has been obtained with the help of theoretical works developed by Bardeen-Shockley[15] and Herring-Vogt,[16] as well as the experimental works by Bagguley *et al.*[17] and by Ito *et al.*[18] In order to make a quantum-mechanical calculation of the conductivity, modification[19] of Ito's formula has been made, with the k_H-broadening[11] being taken into account.

§ 2. Experimental

For the experimental study of solid which is uniaxially compressed, it is required to have a precise stress apparatus and samples having the shape of strictly rectangular parallelepiped. Wafers with [110] surfaces are cut from a single crystal ingot to a thickness of about 1.0 mm by a conventional slicing machine furnished with a diamond blade. The sliced wafer is fixed on a flat glass plate with shellac and the glass plate is further mounted on an unglazed ceramic base with sealing wax. The pasted wafer is cut through the glass base by the diamond blade with extreme care. In this way a rectangular rod is obtained whose size is $11.0\times1.0\times1.0$ mm^3. It is then pasted with fine sealing wax on the surface of a polishing matrix. The latter is made of massive brass block at the precision of 1/1000 so that polished surfaces are necessarily made parallel to each other. Finally this rod is polished with diamond paste on silk cloth and etched with *CP4* solution for a few minutes.

It has been difficult to apply uniaxial compression in a homogeneous and reversible way, since the space restriction is very acute in such a low temperature measurement under a magnetic field. Especially the parallel squeezer, in which the direction of the compressive force is parallel to the horizontal plane within which the magnetic field is rotated, is more difficult to produce than the perpendicular squeezer, in which the relevant directions are perpendicular to each other. In Figs. 1 and 2 the parallel squeezer system is shown. Its residual friction is very small. Stress as high as 2×10^3 kg/cm^2 is obtained through a lever arm having a mechanical advantage of 2.79 and making the cross section of the sample as small as 5×10^{-3} cm^2. The essential part of the squeezer consists of brass piston and small non-magnetic stainless-steel balls which are used to change the direction of force by 90°. In the course of changing stress, the [110] plane of the sample is always kept strictly within the plane of the magnetic field rotation.

In order to study hole scattering by lattice vibrations, it is required to have extremely pure samples, for neutral impurities have strong effects on

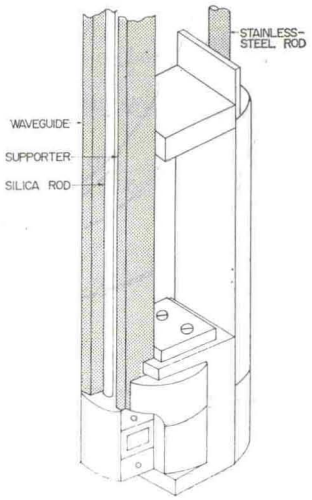

Fig. 1. Outer view of the squeezer head.

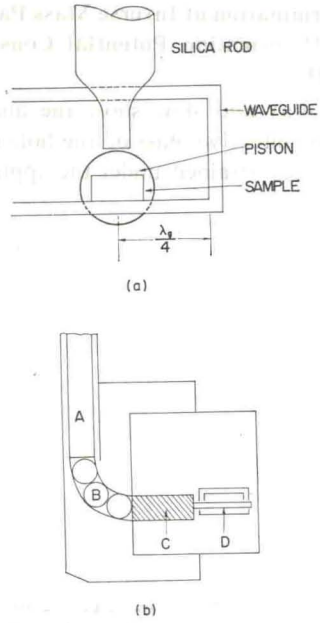

Fig. 2(a). Alignment of the piston, sample and silica rod at the central part of the parallel squeezer.
(b). Local details of the mechanism of the squeezer.

A: Pushing rod
B: Stainless-steel balls
C: Piston (shaded part)
D: Sample through the waveguide

the linewidth.[17,20,21] Samples employed are ultra-high pure germanium (70 ohm-cm) kindly supplied by Dr. H. Yonemitsu at the Tokyo Shibaura Electric Company. Balanced bridge non-resonant superheterodyne spectrometers operating at 35 GHz and 70 GHz have been used. These simplified detection systems make it possible to operate at less than 10^{-7} watt with quite a tolerable signal-to-noise ratio. Carriers are generated by white light illumination from an 8V–50W projecter lamp and through a Toshiba infrared glass filter IRD–1A, which is to cut the wavelength less than 0.9μ off.

The light intensity is weakened by operating the lamp at 1.5∼4V and using an optical iris to avoid the broadening due to carrier-carrier interactions.[22] The sample is directly immersed in the liquid helium bath.

A typical feature of the absorption lines is shown in Fig. 3.

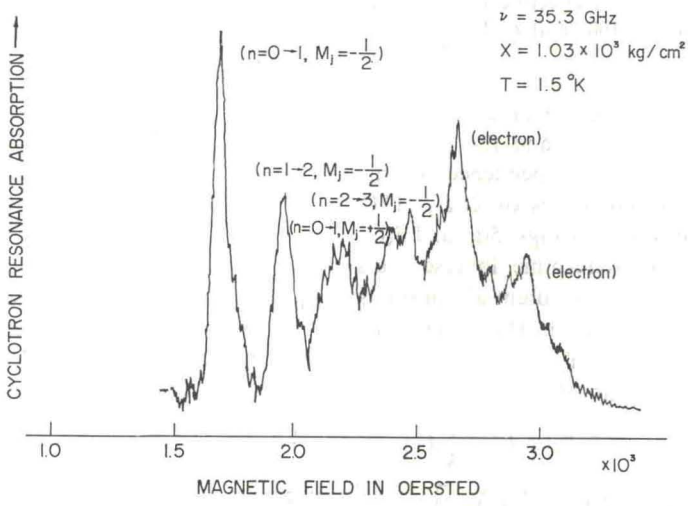

Fig. 3. A typical quantum spectrum for H, $\chi // \langle 111 \rangle$.

§ 3. Determination of Inverse Mass Parameters and Deformation Potential Constants D_u and $D_{u'}$

Figures 4(a) and 4(b) show the angular dependence of effective mass of the hole cyclotron resonance lines obtained under the application of high stress, where the angle θ taken along the abscissa is between the stress and the magnetic field directions. The stress dependences of the effective mass in the geometries of χ, $H//\langle 111\rangle$ and χ, $H//\langle 100\rangle$ are shown in Figs. 5(a) and 5(b), respectively. One can determine inverse mass parameters and deformation potential constants from the above data. The strain Hamiltonian H_ε constructed by Kleiner-Roth[23] in terms of the angular momentum operator J is

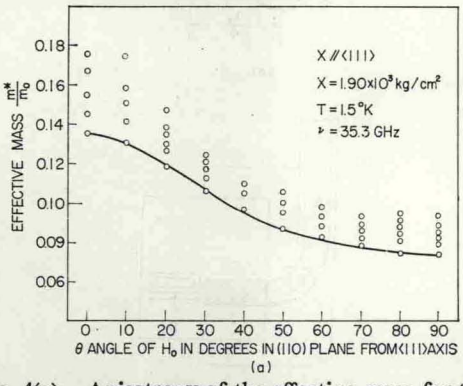

Fig. 4(a). Anisotropy of the effective mass for the hole resonance with $\chi//\langle 111\rangle$ and $\chi=1.9\times10^8$ kg/cm².

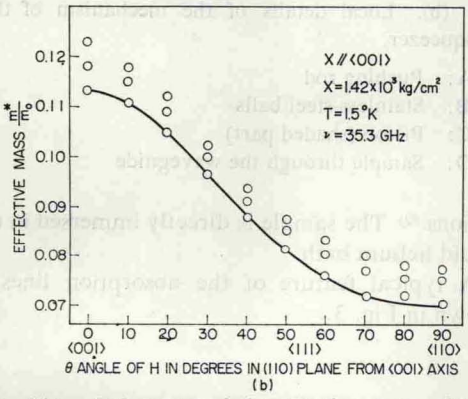

Fig. 4(b). Anisotropy of the effective mass of the hole resonance with $\chi//\langle 100\rangle$ and $\chi=1.42\times10^8$ kg/cm².

$$H_\varepsilon=D_d^{\Gamma}(e_{xx}+e_{yy}+e_{zz})+\frac{2}{3}D_u\left[\left(J_x^2-\frac{1}{3}J^2\right)e_{xx}+\left(J_y^2-\frac{1}{3}J^2\right)e_{yy}+\left(J_z^2-\frac{1}{3}J^2\right)e_{zz}\right]+\frac{2}{3}D_{u'}[\{J_xJ_y\}e_{xy}+\{J_yJ_z\}e_{yz}+\{J_xJ_z\}e_{zz}]\ ; \qquad (3.1)$$

where $e_{xx}, \cdots, e_{xy}, \cdots$ are strain components while D_d^{Γ}, D_u and $D_{u'}$ are the valence band de-

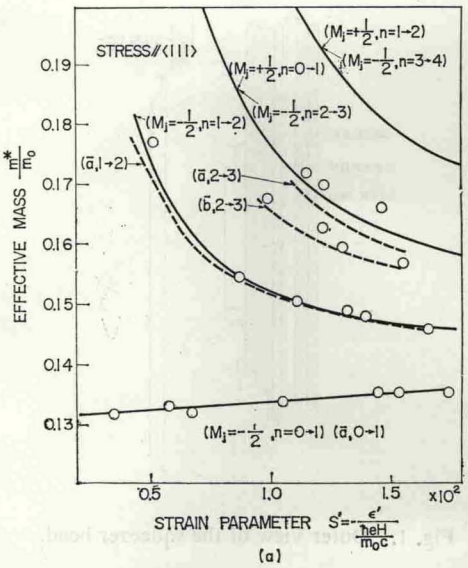

Fig. 5(a). Dependence of the effective mass of the hole cyclotron resonance lines on strain parameter[12] s' for χ, $H//\langle 111\rangle$ and 35 GHz at 1.5°K. The solid and dashed curves refer to the theoretical calculations given by the second order perturbation and by matrix diagonalization, respectively.

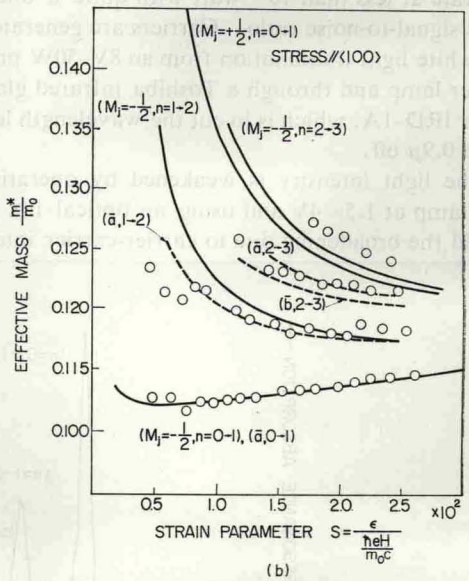

Fig. 5(b). Dependence of the effective mass of the hole cyclotron resonance lines on strain parameter s for χ, $H//\langle 100\rangle$ and 35 GHz at 1.5°K.

formation potential constants. The effective mass Hamiltonian H_k for $\boldsymbol{k}\cdot\boldsymbol{p}$ perturbation is[4]

$$\begin{aligned} H_k=&A(k_x^2+k_y^2+k_z^2)-B\left[k_x^2\left(J_x^2-\frac{1}{3}J^2\right)\right.\\ &\left.+k_y^2\left(J_y^2-\frac{1}{3}J^2\right)+k_z^2\left(J_z^2-\frac{1}{3}J^2\right)\right]\\ &-\frac{2}{3}N[\{k_xk_y\}\{J_xJ_y\}+\{k_xk_z\}\{J_xJ_z\}\\ &+\{k_yk_z\}\{J_yJ_z\}]\ ; \end{aligned} \tag{3.2}$$

Under high stress, one is able to treat H_k in the Hamiltonian $H=H_e+H_k$ as the perturbation to H_e. It has been calculated to second order by Hasegawa.[11] The values of A, B, N, D_u and $D_{u'}$ can be so determined as the experimental and theoretical effective masses agree most nicely with each other over the angle θ between the stress and magnetic field directions for the transition ($n=0\rightarrow1$) and over the stress for those ($n=0\rightarrow1$ and $n=1\rightarrow2$). Use is made of the relation

$$\left(\frac{1}{m^*}\right)^2=\frac{\cos^2\theta}{m_\perp{}^2}+\frac{\sin^2\theta}{m_\perp m_{/\!/}}\ ; \tag{3.3}$$

whence we treat two cases of stress direction.

Case I $\chi//\langle111\rangle$

In eq. (3.3) we put

$$m_\perp=\frac{1}{A-\frac{N}{6}(1-4x)} \quad\text{and}\quad m_{/\!/}=\frac{1}{A+\frac{N}{3}(1-4x)}$$

for the transition ($n=0\rightarrow1$, $M_j=-\frac{1}{2}$);

where $x=\dfrac{\varepsilon'}{\lambda}$, $\varepsilon'=\dfrac{D_{u'}\chi}{3c_{44}}$ and λ is the spin-orbit coupling constant. For a particular orientation $H//\langle111\rangle$, we find the expression of effective mass for the transition $n\rightarrow n+1$:

$$\frac{m^*}{m_0}=\frac{1}{A-\frac{N}{6}(1-4x)-\dfrac{\left(B^2+\frac{2N^2}{9}\right)n}{\dfrac{4\varepsilon'}{\dfrac{\hbar eH}{m_0c}}}}\ ,$$

for $M_j=-\dfrac{1}{2}$, (3.4)

and

$$\frac{m^*}{m_0}=\frac{1}{A-\frac{N}{6}(1-4x)-\dfrac{\frac{1}{2}\left(B^2+\frac{2N^2}{9}\right)+\frac{1}{4}\left(B^2+\frac{2N^2}{9}\right)n}{\dfrac{\varepsilon'}{\dfrac{\hbar eH}{m_0c}}}}\ ,$$

for $M_j=+\dfrac{1}{2}$.

Case II $\chi//\langle100\rangle$

We put

$$m_\perp=\frac{1}{A-\frac{B}{2}(1-4x)} \quad\text{and}\quad m_{/\!/}=\frac{1}{A+B(1-4x)}\ ,$$

in eq. (3.3);

where $x=\dfrac{\varepsilon}{\lambda}$ and $\varepsilon=\dfrac{2D_u\chi}{3(c_{11}-c_{12})}$.

For $H//\langle100\rangle$, we have

$$\frac{m^*}{m_0}=\frac{1}{A-\frac{1B}{2}(1-4x)-\dfrac{\frac{3}{8}\left\{\left(B\pm\frac{1}{3}N\right)^2+\left(B^2+\frac{N^2}{9}\right)n\right\}}{\dfrac{\varepsilon}{\dfrac{\hbar eH}{m_0c}}}}\ ,$$

according as $M_j=\pm\dfrac{1}{2}$. (3.5)

Both in Figs. 4 and 5, the theoretical variations of the effective masses are given by the solid lines. We may note the peak ($n=2\to3$, $M_j=-\frac{1}{2}$) coincides with that of ($n=0\to1$, $M_j=+\frac{1}{2}$) in the case χ, $H//\langle111\rangle$ in eq. (3.4). Agreement between theory and experiment is not so good for large quantum numbers and in the low stress region, for the second order perturbation becomes questionable on one hand while the resolution of the lines becomes worse. With a moderate stress and at temperature below 4.2°K, population of carriers on the levels $M_j=\pm\frac{3}{2}$ is small and can be safely neglected in the present analysis.

In the treatment given so far, the Zeeman shift of the energy has been neglected, because it is smaller than the strain shift by an order of magnitude for the strain of 1.0×10^{-3}. An extra term associated with this Zeeman shift, however, should be taken into account in the low strain region as well as for large quantum numbers. We may calculate the energy levels by a different approach; *i.e.*, diagonalization of the total Hamiltonian $H=H_e+H_k+H_{\text{Zeeman}}$, under the assumption $B=N/3$.[19] The value for g-factor (2κ) can be obtained from Figs. 5(a) and 5(b) through fitting the diagonalization curves (dashed) with the experimental data. In the diagonalization approach, the M_j classification employed so far is replaced by the notations $a^{\pm}$ and $b^{\pm}$ in accordance with Gurgenishivili.[24]

§ 4. Linewidth of the Quantum Line

In the case that carriers are scattered by the thermal lattice vibrations, Bardeen and Shockley[15] made a theoretical calculation for mobilities of electrons and holes in nonpolar crystals. The scattering probability was calculated for isotropic phonons ($c_{44}=\frac{1}{2}(c_{11}-c_{12})$) by the deformation potential method, in which the carriers in a strained lattice feel a local energy disturbance δE proportional to the strain components e_{ij}; *i.e.*,

$$\delta E=\sum_{ij}\Xi_{ij}e_{ij}\,. \tag{4.1}$$

Here Ξ_{ij} is the deformation potential constant for electron. Herring and Vogt extended the above method to the case of many valley semiconductors with an approximate anisotropic dispersion relation for phonons.[16] The relaxation time can be simplified in the ellipsoidal constant energy surface. In order to calculate the relaxation time of holes in germanium under uniaxial compression, it is necessary to construct an interaction term analogous to eq. (4.1). When the uniaxial stress is applied along the $\langle111\rangle$ direction, the corresponding interaction Hamiltonian is given by eq. (3.1). It is a good approximation to solve eq. (3.1) through the second order perturbation in the high stress limit. The reason why we can use the Herring-Vogt method is that the originally warped energy surfaces for holes, under the application of uniaxial stress, become nearly ellipsoidal around the axis of stress, thus simulating themselves to those for electrons. The final result is given in terms of the usual second rank tensor:

$$\mathbf{D}=\begin{pmatrix} D_d^V & -\frac{1}{3}D_{u'} & -\frac{1}{3}D_{u'} \\ -\frac{1}{3}D_{u'} & D_d^V & -\frac{1}{3}D_{u'} \\ -\frac{1}{3}D_{u'} & -\frac{1}{3}D_{u'} & D_d^V \end{pmatrix}. \tag{4.2}$$

It is worth noting that eq. (4.2) does not contain the parameter D_u, that is, it is described only by two parameters D_d^V and $D_{u'}$. The corresponding expression for the relaxation time of hole becomes

$$\frac{1}{\tau_\perp}=(3\pi Ck_BT\varepsilon^{1/2}/Vc_l)(\xi_\perp D_d^{V^2}+\eta_\perp D_d^V D_{u'}+\zeta_\perp D_{u'}^2); \tag{4.3}$$

where

$$C=(m_\perp^2 m_{//})^{1/2}\,V/2^{3/2}\pi^2\hbar^4\,,$$

$$c_l=c_{12}+2c_{44}+\frac{3}{5}c^*$$

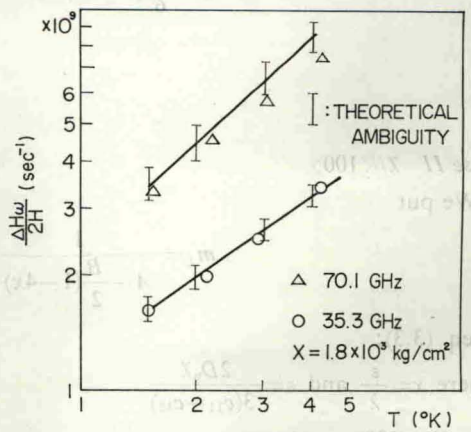

Fig. 6. Temperature dependence of linewidth of the hole cyclotron transition ($n=0\to1$, $M_j=-\frac{1}{2}$) under the conditions shown. The theoretical curves are fitted to the experimental values at 1.5°K. Theoretical ambiguity arises from the difficulty of determining the positions to measure the half-width; namely, the resonance lines may oscillate in the high magnetic field region, owing to the terms $\sum_n(E-n\eta)^{-1/2}$ in eq. (4.4).

and

$$c^*=c_{11}-c_{12}-2c_{44}$$

with

$$\xi_\perp=1.4,\ \eta_\perp=0.67 \text{ and } \zeta_\perp=0.38$$

in the case χ, $H//\langle 111\rangle$; ε is the energy of a hole and V the volume of the crystal. The coefficients $\xi_\perp$, $\eta_\perp$ and $\zeta_\perp$ are anisotropy parameters which depend on the effective mass ratio $m_\perp/m_\parallel$.

The temperature dependence of the linewidth measured under the compression of 1.8×10^3 kg/cm^2 for the cyclotron transition ($n=0\to1, M_j=-\frac{1}{2}$) is shown in Fig. 6 between 1.5 and 4.2°K together with the theoretical line. Since $\varepsilon\propto T^{1/2}$ in thermal equilibrium, one may expect from eq. (4.3) $1/\tau_\perp\propto T^{3/2}$ as in the case for electrons. One finds, however, the linewidth varies approximately linearly with temperature at the frequency of 70.1 GHz, though the temperature dependence becomes somewhat less steep in the case of 35.3 GHz. This result strongly suggests an appreciable contribution of k_H broadening to the line. In fact, it is easy to show that the resonance linewidth varies linearly with temperature if we assume the transition to occur between two parabolic Landau levels with different curvatures.

One is now to analyze the linewidth. For the valence band problem one has to modify Ito's calculation of conductivity[18] by taking the $\Delta\omega(k_H)$ shift into account. In the case $\chi//\langle111\rangle$ and for the transition ($n=0\to1$, $M_j=-\frac{1}{2}$), the relevant conductivity expression is given by

$$\sigma(X,\eta)=\int_0^\infty dE E^{-1/2}\frac{\{(E+\eta)^{-1/2}+2\sum_n(E-n\eta)^{-1/2}\}^{-1}e^{-(E+\alpha E)}}{1+16Y^2[\eta\{E+\eta)^{-1/2}+2\sum_n(E-n\eta)^{-1/2}\}]^{-2}}\ ; \tag{4.4}$$

where

$$Y=(X-\Delta\omega(k_H))\tau\ ,$$

$$X=\omega-\omega_0\ ,$$

$$\Delta\omega(k_H)=\frac{eH}{\hbar^2c}k_H^2\left(2B^2+\frac{1}{9}N^2\right)\Big/\Delta E$$

and

$$\alpha=\frac{2B^2+\frac{1}{9}N^2}{2\left(A+\frac{1}{3}N\right)\left(A-\frac{1}{6}N\right)}\frac{\hbar\omega_0}{\Delta E}$$

with

$$\eta=\frac{\hbar\omega_0}{k_BT},\quad E=\frac{\hbar^2k_H^2}{2m_\parallel k_BT}\ \text{ and }\ \Delta E=2\varepsilon'\ .$$

In this approximation, we have considered the relaxation process only for the $M_j=-\frac{1}{2}$ ladder set without taking the effect of nonparabolicity into account. Since k_BT, $\hbar\omega_c\ll\Delta E$, the phonon-induced transition probability from $M_j=-\frac{1}{2}$ to $M_j=+\frac{1}{2}$ or to $M_j=\pm\frac{3}{2}$ is considered quite small, and higher order terms can also be neglected to calculate the $\Delta\omega(k_H)$ shift. The so-called reduced linewidth X_{half} is given by

$$X_{half}=X_1-X_2=\tau_\perp\Delta\omega \text{ (half-width)}\ . \tag{4.5}$$

Here X_1 and X_2 should satisfy the equation

$$\sigma(X_i,\eta)=\frac{1}{2}\sigma(X_{max},\eta),\ i=1 \text{ and } 2\ . \tag{4.6}$$

By adjusting the theoretical value of X_{half} to be equal to the experimental one at 1.5°K (see Fig. 7), we obtain $D^2=30$ (eV)^2, where $D^2=1.4D_d^{V2}+0.67D_d^VD_{u'}+0.38D_{u'}^2$. The D^2 value obtained here is somewhat smaller than that obtained in the previous work,[19] in which the estimation of $\Delta\omega(k_H)$ as well as employed values of the band parameters were inadequate. For solving eq. (4.4) numerically, the NEAC 2200-500 computer has been used. Figure 8 shows that stress dependence of the linewidth at 1.5°K. We have a nice fit of experimental data with calculation. D_d^V is now obtainable from eq. (4.3), using the values of $D_{u'}$ and D^2. Solution of the quadratic equation yields $D_d^V=-5.2$ or $+3.3$ eV. Choice between these two roots is a difficulty. It should be made not to contradict with experimental results for the variation of the energy gap against hydrostatic volume change. A little more discussion will be made in the next section.

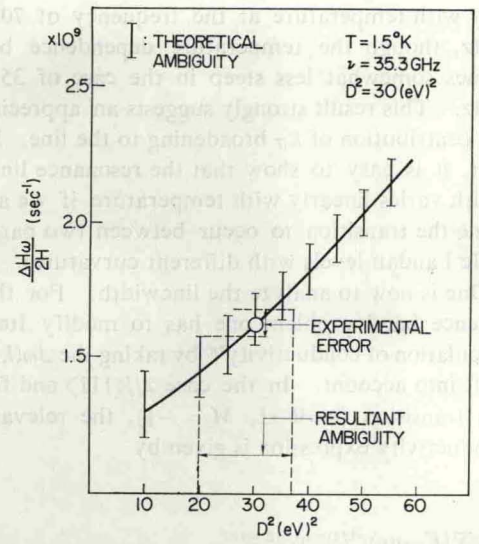

Fig. 7. Dependence of the half-width $\frac{\Delta H\omega}{2H}$ on D^2.
The solid curve refers to the theoretical calculation for χ, $H//\langle 111\rangle$ and 35 GHz at 1.5°K.

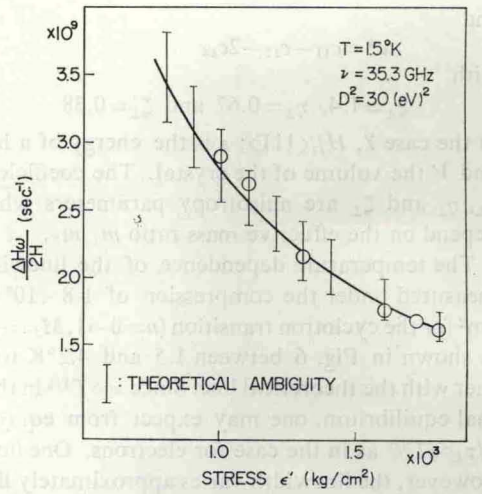

Fig. 8. Stress dependence of half-width of the hole cyclotron transition ($n=0\to1$, $M_j=-\frac{1}{2}$) under the conditions shown.

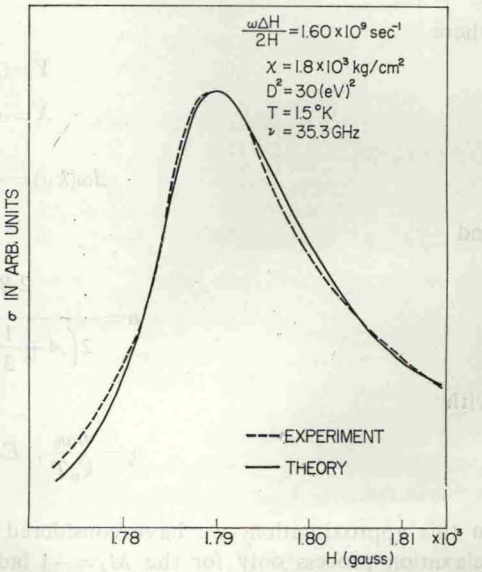

Fig. 9. Theoretical and experimental lineshapes for the transition line ($n=0\to1$, $M_j=-\frac{1}{2}$).

§ 5. Discussions

1) Characters of the quantum lines

For measuring the width of a quantum line, resolution is essential. The condition $|\omega_{c1}-\omega_{c2}|>\Delta\omega$ (we shall call this the secondary condition) is required on top of the ordinary condition for observability of cyclotron resonance; *i.e.*, $\omega_{c1}\tau$ and $\omega_{c2}\tau$ be greater than unity (we may call this the primary condition). Here, ω_{c1} and ω_{c2} are angular frequencies at adjacent peaks, while $\Delta\omega$ the linewidth. In our experiments the maximum value of $|\omega_{c1}-\omega_{c2}|/\Delta\omega$ is 10. In order to get an optimum resolution as well as signal-to-noise ratio, one should control the stress very carefully. At moderate stress, both $|\omega_{c1}-\omega_{c2}|$ and $\Delta\omega$ are nearly inversely proportional to the stress (see Fig. 5(a) and Fig. 8). At high stress, dependence of the former on stress does not change, while the latter approaches a limiting value. The resolution of lines then becomes worse as the stress is increased. The fact that we cannot observe the higher quantum lines with enough resolution is explained by the reason that $\Delta\omega$ gets larger as the quantum number is increased and thereby the secondary condition is no longer satisfied. This is because the higher energy levels are more strongly coupled with the bands $M_j=\pm\frac{3}{2}$.

The lineshape of a quantum line differs from the usual Lorentzian shape. Because of the $\Delta\omega(k_H)$ contribution, it has an asymmetric structure as is characterized by a shoulder on the high magnetic field side. One can see this feature in eq. (4.4) and Fig. 9.

In Fig. 3, quantum lines are distinct up to fairly high n values. Though the higher states have smaller populations, the oscillator strength which is proportional to $(n+1)$ makes up for that.

2) Inverse mass parameters A, B, N, g-factor (2κ) and shear deformation potential constants D_u and $D_{u'}$

The values of the inverse mass parameters A, B, and N as well as those of the shear deformation potential constants D_u and $D_{u'}$ can be deter-

Table (3-1). The valence band parameters given by experiments. (A, B, N) and $(D_u, D_{u'}, D_d{}^V)$ are given in units of $\hbar^2/2m_0$ and eV, respectively.

Group	$-A$	$-B$	$-N$	κ	D_u	$D_{u'}$	$D_d{}^V$
Dexter *et al.*[a]	13.1 ±0.4	8.3 ±0.6	32.1 ±0.5	3.9			
Levinger *et al.*[b]	13.27	8.63	33.6				
Goodman[c], Fletcher *et al.*[d]	13.21	8.56	33.36	3.9			
Okazaki[e], Hensel[f]	13.2	8.12	33.72	3.9			
Hensel[g]	13.38 ±0.02	8.60 ±0.04	34.08 ±0.12	3.60 ±0.04		3.91 ±0.25	
Otsuka *et al.*[h]					4.2 ±0.2	4.9 ±0.5	
Hall[i]					3.15	6.1 ±1.3	
Glass[j]					3.1 ±0.5	4.1 ±0.5	
Balslev[k]					2.7 ±0.5	3.2 ±0.4	
Present	13.50 ±0.05	8.80 ±0.09	35.20 ±0.23	3.9	3.14 ±0.20	4.00 ±0.20	$-5.2^{-0.5}_{+1.0}$ or $3.3^{+0.5}_{-1.0}$

a. R.N. Dexter, H.J. Zeiger and B. Lax: Ref. 1).
b. B.W. Levinger and F.R. Frankl: J. Phys. Chem. Solids **20** (1961) 281.
c. R.R. Goodman: Ref. 7).
d. R.C. Fletcher, W.A. Yager and F.R. Merritt: Ref. 6).
e. M. Okazaki: Ref. 9).
f. J.C. Hensel: Ref. 8).
g. J.C. Hensel: Ref. 14).
h. E. Otsuka, K. Murase and H. Fujiyasu: Ref. 13).
i. J.J. Hall: Ref. 25).
j. A.M. Glass: Canad. J. Phys. **43** (1965) 12.
k. I. Balslev: Phys. Rev. **143** (1966) 636.

mined very accurately from the first and second quantum lines, using Hasegawa's second order perturbation method which takes the spin-orbit split-off band into account. For determining κ, the above parameters and the assumption that $B-N/3\cong 0$ are used. Values of D_u and $D_{u'}$ obtained so far are to fall around 4 and 3 eV, respectively, except for Hall's data[25] for D_u (Table (3-1)). The values $D_{u'}=4.9$ and $D_u=4.2$ (eV) given by our previous experiments are a little larger than the present ones. In the past, a perpendicular squeezer ($H\perp\chi$) was used. The calibration of the stress was indeed accurate, but the subsequent analysis was difficult because of the poor resolution of the second quantum line.

Kohn[26] estimates the H_2 band parameter for Ge to fall in the range $0>H_2\geq -0.5$. The present result satisfies this requirement; namely $H_2=-0.41$. For D_u and $D_{u'}$ there exists a theoretical calculation by Goroff and Kleinman for Si.[27] No calculation has been available for Ge. One might see some significance in the ratio $D_{u'}/D_u$. According to Goroff and Kleinman, the ratio becomes 1.2 for Si. The present work for Ge gives $D_{u'}/D_u=1.3$, which is very close to the predicted value for Si.

3) Comparison of the value of D_d^V with those derivd by indirect method

The present work derives the D_d^V value solely from the same valence band cyclotron resonance measurement. One may, however, also find the quantity in an indirect way, which combines the hydrostatic compression data with the information of the conduction band deformation potential constants. In order to see how effective the latter method is, we shall give some qualitative discussions below.

The dependence of the band gap energy $E_g(L_1-\Gamma_{25}')$ on deformation is given by the relation

$$\mathrm{d}E_g/\mathrm{d}\ln V=\Xi_d+\Xi_u/3-D_d^V\ . \qquad (5.1)$$

The value of $\mathrm{d}E_g/\mathrm{d}\ln V$ has been measured by a number of workers. Experimental data prior to 1960 are summarized by Keyes and grouped into

two branches, the first branch centered around −3.8 eV while the second around −5.7 eV.[28] Recently Balslev adds another precise set of data.[29] As for the set of Ξ_u and Ξ_d, perhaps most reliable data are obtainable from cyclotron resonance experiments[18,30,31] and their values are given in Table (5-1). One can then derive the value of D_d^V from eq. (5.1) and the data in Table (5-1). The results are shown in Table (5-2). We get a considerable scatter of values for D_d^V from various possible combinations of the available data. Almost in every case, however, one finds D_d^V negative. One is thus inclined to choose the value −5.2 eV rather than +3.3 eV. The absolute value yet seems a little bit too large. Indeed the present method deduces the D_d^V value solely from the same experimental series of cyclotron resonance. But one should admit the large ambiguity inherent to D^2 which is difficult to overcome by experimental accuracy at present. The parameters in eq. (5.1) used to derive D_d^V, on the other hand, can be determined, in principle, as accurately as we wish. Especially the recent precise determination of Ξ_u and Ξ_d,[31] in the present authors' opinion, is quite encouraging for the use of eq. (5.1). A final conclusive value of $dE_g/d\ln V$ would then lead to a more realistic value of D_d^V than the one obtained in this work. More elaborate works both experimental and theoretical would be required to settle the problem.

Table (5-1). The deformation potential constants (Ξ_u and Ξ_d) as well as the energy shift of the conduction band.

Group	Ξ_u(eV)	Ξ_d(eV)	$\Xi_d+\Xi_u/3$ (eV)
Bagguley *et al.*[a]	16.6	−11.3	−5.8
Ito *et al.*[b]	18.7	−10.5	−4.3
Murase *et al.*[c]	19.3	−12.3	−5.9

[a]. Ref. 30). The values tabulated here are different from the original ones given in ref. 30), since the method of average for electron scattering is modified in accordance with Gold *et al*: Phys. Rev. **103** (1956) 1250.
[b]. Ref. 18).
[c]. Ref. 31).

Table (5-2). Scatter of the D_d^V values derived indirectly from eq. (5.1) with the help of the conduction band deformation potential constants obtained by three groups in Table (5-1). In the first column, three representative values of $dE_g/d\ln V$ are given to start with. Case *a*, Case *b* and Case *c* correspond to *a*, *b* and *c* in Table (5-1), respectively.

$dE_g/d\ln V$ (eV)	Case *a* (eV)	Case *b* (eV)	Case *c* (eV)
−3.8[28]	−2.0	−0.5	−2.1
−5.7[28]	−0.1	1.4	−0.2
−3.2[29]	−2.6	−1.1	−2.7

In summary, it should be stressed that though the accurate determination of the band parameters of the valence band of germanium is difficult because of the Γ_{25}' degeneracy, the present method which utilizes cyclotron resonance technique associated with uniaxial stress makes it possible to determine them much more accurately than the previous works. The newly obtained set of parameters will no doubt facilitate the future discussions of the dynamics of the holes in germanium.

Acknowledgements

The authors wish to express their sincere gratitude to Professor H. Kawamura for his continual interest, fruitful advice and encouragements.

They are much indebted to Dr. H. Yonemitsu of the Toshiba Electric Co. Ltd. for supplying pure germanium single crystals.

Discussions and critical comments by Professor H. Hasegawa in theoretical aspects have been most helpful and are so deeply appreciated.

They express their thanks to Dr. T. Ohyama for discussions and cooperation in carrying out this work.

References

1) R.N. Dexter, H.J. Zeiger and B. Lax: Phys. Rev. **104** (1950) 637.
2) G. Dresselhaus, A.F. Kip and C. Kittel: Phys. Rev. **92** (1953) 827.
3) J.M. Luttinger and W. Kohn: Phys. Rev. **97** (1955) 869.
4) J.M. Luttinger: Phys. Rev. **102** (1956) 1030.
5) R.F. Wallis and H.J. Bowlden: Phys. Rev. **118** (1960) 456.
6) R.C. Fletcher, W.A. Yager and F.R. Merrit: Phys. Rev. **100** (1955) 747.
7) R.R. Goodman: Phys. Rev. **122** (1961) 397.
8) J.C. Hensel: *Rep. Int. Conf. Phys. Semiconductors, Exeter* (1962) p. 281.
9) M. Okazaki: J. Phys. Soc. Japan **17** (1962) 1865.
10) J.C. Hensel and G. Feher: Phys. Rev. **129** (1963) 1041.
11) H. Hasegawa: Phys. Rev. **129** (1963) 1029.
12) J.C. Hensel: Solid State Commun. **4** (1966) 231.

13) E. Otsuka, K. Murase and H. Fujiyasu: Phys. Letters **21** (1966) 284.
14) J.C. Hensel: Phys. Rev. Letters **21** (1968) 983.
15) J. Bardeen and W. Shockley: Phys. Rev. **80** (1950) 72.
16) C. Herring and E. Vogt: Phys. Rev. **101** (1956) 944.
17) D.M.S. Bagguley, R.A. Stradling and J.S.S. Whiting: Proc. Roy. Soc. (GB) **262** (1961) 340 and 365.
18) R. Ito, M. Fukai and Imai: *Proc. Intern. Conf. Physics Semiconductors, Kyoto, 1966*, J. Phys. Soc. Japan **21** (1966) Suppl. p. 357.
19) H. Fujiyasu, K. Murase and E. Otsuka: Phys. Letters **A27** (1968) 597.
20) M. Fukai, H. Kawamura, K. Sekido and I. Imai: J. Phys. Soc. Japan **19** (1964) 30.
21) E. Otsuka, K. Murase and J. Iseki: J. Phys. Soc. Japan **21** (1966) 1104.
22) H. Kawamura, H. Saji, M. Fukai, K. Sekido and I. Imai: J. Phys. Soc. Japan **19** (1964) 288.
23) W.H. Kleiner and L.M. Roth: Phys. Rev. Letters **2** (1959) 334.
24) G.E. Gurgenishvili: Soviet Physics-Solid State **5** (1964) 1510.
25) J.J. Hall: Phys. Rev. **128** (1962) 68.
26) Cited in the paper by K. Suzuki, M. Okazaki and H. Hasegawa: J. Phys. Soc. Japan **19** (1964) 930.
27) I. Goroff and L. Kleinman: Phys. Rev. **132** (1963) 1080.
28) R.W. Keyes: *Solid State Physics* ed. F. Seitz and D. Turnbull (Academic Press, New York and London, 1960) Vol. 11, p. 149.
29) I. Balslev: Phys. Letters **24** (1967) 113.
30) D.M.S. Bagguley, D.W. Flaxen and R.A. Stradling: Phys. Letters **1** (1962) 111.
31) K. Murase, K. Enjouji and E. Otsuka: in preparation.